SANDIA REPORT

SAND2001-1685
Unlimited Release
Printed June 2001

Analysis of Plasma Dust Particle Crystals Confined within a Potential Well

Merle E. Riley and Gregory A. Hebner

Prepared by
Sandia National Laboratories
Albuquerque, New Mexico 87185 and Livermore, California 94550

Sandia is a multiprogram laboratory operated by Sandia Corporation,
a Lockheed Martin Company, for the United States Department of
Energy under Contract DE-AC04-94AL85000.

Sandia National Laboratories

Issued by Sandia National Laboratories, operated for the United States Department of Energy by Sandia Corporation.

Available to DOE and DOE contractors from
U.S. Department of Energy
Office of Scientific and Technical Information
P.O. Box 62
Oak Ridge, TN 37831

Telephone: (865)576-8401
Facsimile: (865)576-5728
E-Mail: reports@adonis.osti.gov
Online ordering: http://www.doe.gov/bridge

Available to the public from
U.S. Department of Commerce
National Technical Information Service
5285 Port Royal Rd
Springfield, VA 22161

Telephone: (800)553-6847
Facsimile: (703)605-6900
E-Mail: orders@ntis.fedworld.gov
Online order: http://www.ntis.gov/ordering.htm

SAND2001-1685
Unlimited Release
Printed June 2001

Analysis of Plasma Dust Particle Crystals Confined within a Potential Well

Merle E. Riley and Gregory A. Hebner
Plasma Sciences Department
Sandia National Laboratories
P.O. Box 5800
Albuquerque, NM 87185-1423

Abstract

An equation of state is developed for a thin layer of dust particles suspended within a confining potential well generated by a plasma sheath. It is shown that measurements of the velocity of a single particle as it falls into the well, combined with observations of the density, radius, and number of particles in the dust layer, can give information about the pair-wise interaction of the particles, a point of scientific interest. We also demonstrate that the observation of Brownian motion can potentially be used to deduce properties of the confining potentials and dust temperature.

1. Introduction

This report will make use of some of the results of an earlier report on plasma dust dynamics.[1] In this report we analyze the compression of a single layer of dust particles subject to a radial confining force. One can picture the confinement of the particles as the settling of particles into the bottom of a geometric "bowl," which is approximately parabolic. Whether the downward force is dominated by gravity or by ion wind effects, the important point is that we can determine the shape of the potential from observations of the dynamics of a single particle as it falls into the potential well. This shape will then determine the radial component of the force applied to the layer of particles. From this force and the density variation within the particle layer, we can infer information about the pair-wise interaction of the individual particles. It is being assumed that the presence of many particles does not change the basic properties of the plasma in the vicinity of the sheath. As the only purpose here is to present the basis for the analysis, we will not discuss general features or much experimental detail. All of the analysis in this work can be developed from any basic plasma physics text.

One of the important points is that a truly perfect crystal arrangement is metastable when confined in a spatially varying force field. The particles will rearrange immediately into an arrangement that is only locally crystalline. In other words, it is full of defects. However this local amount of crystallinity is sufficient to allow us to characterize the internal energy, pressure, and density of the layer of dust particles at a particular location. The state properties of the dust layer can be related to the pair interactions of the particles, which is the object of investigation.

2. Equations of Motion of Plasma Dust Particles

Typical plasma dust particles are suspended at the bottom of the plasma in a nearly planar region, which suggests that gravity has a dominant role. This is not universally true, but the relevant point is that we can approximate the forces and motion of the particle with gravity defining a vertical axis with rotational symmetry about that axis. Later we will discuss the advantage of confining the dust layer within the shallow concave region of an electrode with a spherically curved surface. This arrangement allows us to eliminate many of the unknown forces from consideration. Consider a system with the z-axis pointed upwards. Newton's equation for a single dust particle is

$$m_d \ddot{\vec{r}} = -\hat{e}_z m_d\, g + q_d \vec{E}_{sh} - m_d \gamma_{gas} \dot{\vec{r}} + \vec{f}_w + \vec{f}_{tp}, \tag{1}$$

where we use "dot notation" to denote time derivatives. z is the dust particle vertical coordinate, m_d is the mass of the dust particle, g is the acceleration of gravity, q_d is the charge on the particle, $\vec{E}_{sh}$ is the plasma sheath electric field at the position of the particle, γ_{gas} is the damping rate (1/s) due to collisions with the neutral gas background, $\vec{f}_w$ is the "wind force" on the particle due to ion flow within the non-uniform plasma sheath, and $\vec{f}_{tp}$ is the thermophoretic force due to temperature asymmetries in the background gas. The wind force includes all electric forces on the particle due to its presence in a non-uniform plasma except those forces isolated in the $q_d\, \vec{E}_{sh}$ term. We will use SI units unless otherwise noted. It is seen that g and γ_{gas} are positive constants. q_d, $\vec{f}_w$, $\vec{f}_{tp}$, and $\vec{E}_{sh}$ are all possibly functions of $\vec{r}$ and the particle velocity $\dot{\vec{r}}$.

2.A Forces on particle due to neutral gas background

The damping coefficient is derived by a gas-kinetic analysis. The result for the force acting on a spherical dust particle due to specular reflection of the gas species is[2]

$$\vec{f}_{gas} \approx -\tfrac{4}{3}\pi a^2 m_{gas}\, n_{gas}\, v_{Tgas}\, \vec{v}_d, \tag{2}$$

where $\vec{v}_d = \dot{\vec{r}}$ is the particle velocity relative to the stationary gas and $v_{Tgas} = (8kT_{gas}/\pi\, m_{gas})^{1/2}$ is the thermal velocity (mean speed) of the gas atoms. The particle radius is denoted as a. The damping coefficient is

$$\gamma_{gas} = \tfrac{4}{3}\pi a^2 m_{gas}\, n_{gas}\, v_{Tgas} / m_d\,. \tag{3}$$

This is appropriate considering the small size of the dust particles and the large mean free path of the gas atoms. Eq.(3) may be rewritten as

$$\gamma_{gas} = \sqrt{\frac{8m_{gas}}{\pi kT_{gas}}}\frac{P_{gas}}{a\rho_d}, \tag{4}$$

where P_{gas} is the gas pressure and ρ_d is the density of the particle. There is some uncertainty in the proper value to use for the damping coefficient because of the unknown elastic and inelastic scattering properties of the gas on the particle surface. We note that the case of complete sticking of the gas on the particle surface would give the identical coefficient as given above.[2] Diffuse elastic scattering would increase γ_{gas} by a factor of $1+\pi/8 = 1.3927$, which we believe to be the realistic value. Complete accommodation of a gas atom on a dust particle at a different temperature T_{surf} would increase the drag by a factor[3] of $1+(\pi/8)\sqrt{T_{surf}/T_{gas}}$, a change that might be important considering the continual delivery of energy to the dust particles in their action as a catalyst for plasma recombination.

The thermophoretic force is complicated by the imprecise knowledge of temperature gradients and non-Maxwellian properties of the gas.[4] The mean free path is always much larger than the particle sizes in our system, but that path may be comparable to the dimensions of the physical boundary separations. The characterization of the thermophoretic forces is ameliorated here by the fact that we can design the system so that this force and the plasma electric force are not crucial to most of the analysis.

2.B Electric field within the plasma sheath

In order to calculate the electric field we would need a reasonably accurate model for the sheath and pre-sheath region. This could even be time dependent for some of the situations of interest, but that is difficult to accomplish. We will use a phenomenologically characterized model for the plasma electric field that incorporates most of the important features leading to dust crystallization and dust particle dynamics.

The experimental situation is that of an azimuthally symmetric system. Anything else, unless restricted to a region of reduced geometry, is too complex to analyze. The field that guides the particles is a surface of revolution about the vertical axis. We will use cylindrical coordinates, *r* and *z*. We assume that the plasma potential in the region of the electrode is dominantly a function of *z* with a small *r*-dependent shift in height. This is expressed as

$$\begin{gathered} \phi(\vec{r}) = \phi(z - h(r))\,, \\ h(r) \approx c\,r^2\,. \end{gathered} \tag{5}$$

The approximation of *h* as quadratic will be introduced later when needed. The constant *c* is related to the radius of curvature of the "confining bowl" by $c = 1/2R_c$. The electric field resulting from the potential in Eq.(5) is found:

$$\vec{E}_{sh}(r,z) = -\,(\hat{e}_z - \hat{e}_r\,h'(r))\,\phi'(z - h(r))\,. \tag{6}$$

The choice of $\phi(z)$ will strongly affect the particle motion in the vertical *z* direction, including the location of the particle equilibrium position. The choice of $h(r)$ will affect the lateral motion of particles that are trapped in the potential minimum, which itself is created by the *z* dependence of all the forces.

We will use a phenomenologically characterized sheath potential for $\phi(z)$. The form for $\phi(z)$ is that of a parabola connected smoothly to an exponential decaying towards the plasma bulk. The position of the joining point, the value of the potential at the electrode relative to the bulk, and the decay constant of the exponential are all independently adjustable and allow one to fit the important features of whatever might be known about the sheath and presheath of the plasma. In the experiments to be discussed later, we will use a curved electrode surface with a geometric radius of curvature, R_c, which we will experimentally verify to be the same as the radius of curvature of the confining region of the conformal plasma sheath.

2.C The ion wind force

The ion wind force on the dust particle is due to the scattering of ions off the dust particle as they flow towards the electrode beyond the sheath. We have previously discussed the cross section that is used here for the momentum transfer.[1] The new point here is that the ions and dust particles are moving in three dimensions and we must obtain the correct vector dependence of the wind force.

First of all we assume that the ion flow velocity, $\vec{v}_{ion} \equiv \vec{v}_{wind}$, is parallel to the electric field within the sheath. This is not a bad assumption, as the ions respond to the field much more rapidly than the particles. Whether the ion flow is collisional (fluid or drift-diffusion) or the ions are in free fall, their motion is dominantly along the electric field vector. Thus the wind force on a stationary dust particle is directed along $\vec{E}_{sh}$ and the force on a moving particle is obtained from the vector addition of the velocities. For example, a moving particle in a stationary ion background has a wind force that opposes the particle velocity. The wind force is given in terms of the momentum-transfer cross section $\sigma_{mt}(v_{rel})$, where v_{rel} is the relative ion-particle velocity,

$$\vec{v}_{rel} = \vec{v}_{ion} - \vec{v}_d \,, \tag{7}$$

by the expression:

$$\vec{f}_w = n_{ion}\, v_{rel}\, m_{ion}\, \vec{v}_{rel}\, \sigma_{mt}(v_{rel}) \,. \tag{8}$$

Because the ion velocity, drift or kinetic, is always much larger than the particle velocity, we can replace $\vec{v}_{rel}$ by $\vec{v}_{ion}$ in most of the analysis. In this case we see that the product $n_{ion}v_{ion}$ in the wind force is just the ion flux Φ_{ion} flowing through the plasma sheath. This is immediately related to the ion current, or to the plasma density and the Bohm velocity.

2.D Charging of particles due to electron and ion impact

We have previously considered the theories available in the literature and selected what would appear to be the most accurate and reasonable.[1] Although we can estimate the equilibrium charge on the particle due to the local plasma environment, it is better to calculate the charge from estimates of the rate of electron and ion impact. In so doing, we will include any time lag in the relation of particle charge to the instantaneous position within the plasma sheath. We will assume that the collisions with the particle result in unit sticking or accommodation on the particle surface. This is not necessarily true, and corrections can easily be made if more information is known about the process. The charging rate of a particle is written in terms of the incident ion and electron currents to the surface:

$$\dot{q}_d = I_i + I_e . \tag{9}$$

The electron current is evaluated in terms of the Boltzmann assumption about the electron distribution function in the sheath and plasma. The local density is related to the bulk (or Bohm point) density by means of the Boltzmann distribution in order to simplify the result:

$$
\begin{aligned}
I_e &= -e4\pi a^2 \Phi_{ed} \\
&= -e4\pi a^2 \tfrac{1}{4} n_e(\vec{r}) v_{Te} \exp\left(e(V_d - \phi(\vec{r})/kT_e\right). \\
&= -e\pi a^2 n_B v_{Te} \exp\left(e(V_d - V_B)/kT_e\right)
\end{aligned}
\tag{10}
$$

Φ_{ed} is the electron flux on the surface, v_{Te} is the electron thermal velocity, $v_{Te} = (8kT_e / \pi m_e)^{1/2}$, and the potential at the Bohm reference point V_B is defined to be zero. Note that the only dynamic dependence remaining in I_e is in the surface potential. The rise in (negative) potential at the dust surface above the local sheath potential is estimated from the capacity relation of a charged sphere:

$$
V_d - \phi(\vec{r}) \approx \frac{1}{4\pi\varepsilon_o} q_d / a \tag{11}
$$

One could treat either V_d or q_d as the unknown property of the particle for the purposes of numerical solution.

The ion current is not so easily approximated due to the ion orbiting. There are many studies of ion capture and scattering from small charged bodies because the physical situation is the same as that of plasma probe analysis. Many of these have been discussed in the context of dust particles. We use the microcanonical distribution function for ions ignoring multiple turning points and absorptive corrections. This limiting case of the complex general theory gives:

$$
\begin{aligned}
I_i &= e\pi a^2 n_i(\vec{r}) v_i(\vec{r}) \left(1 - \frac{e\Delta V}{K_i(\vec{r})}\right) \\
&= e\pi a^2 \Phi_i \left(1 - \frac{e(V_d - \phi(\vec{r})}{K_i(\vec{r})}\right)
\end{aligned}
\tag{12}
$$

ΔV is the fall in potential of an ion as it encounters the particle surface at the local position in the sheath. The ion flux, Φ_i, is constant through the sheath. $K_i(\vec{r})$ is the kinetic energy of the ions at position $\vec{r}$ within the sheath, which can be approximated from the fall through the sheath potential. If we sum the electron and ion currents to zero, we obtain a value for the steady state, equilibrium charge and potential carried by the particle. Eqs.(10) and (12) , due to Mott-Smith and Langmuir, are what are called the orbital motion limited theory of charging,[5] except for our modifications to match to the local potential at the particle position.

Thus all the dynamical forces acting on a dust particle are now known in terms of the plasma properties. These can be used in the Newtonian equation of motion for the particle to observe its trajectory when dropped into the plasma. If we add particle-particle interactions, we are ready to do multiparticle dynamics. For the purposes in this report, however, we will not be looking at particle dynamics except in the equilibrium layer formed with several particles. Nevertheless we will need to have the function $h(r)$ or the quadratic coefficient c characterizing the curvature of the potential field.

3. Energetics of a 2D Confined Disk-Like Particle Layer

The experimental observations are of dust particles that have fallen into the sheath or presheath of the plasma located above a flat electrode. There the dust particles exhibit mostly horizontal motion as they “slide” laterally toward the center of the electrode. In most cases the particles form single layers, and that is the ideal situation that we will address here. In this case we can approximate the equations of motion for the particles to better isolate the lateral forces acting on them.

Consider a particle to be at equilibrium in the curvilinear coordinate measured along the local plasma electric field direction $\hat{E}(r,z)$, which is very close to the vertical direction. This requires that this component of the force is zero. Because the wind force vector closely parallels the electric field vector, we know that only gravity and the viscous forces can act to accelerate or decelerate the particle in the lateral direction perpendicular to $\hat{E}(r,z)$. It is sufficient just to consider the forces of gravity and electric field acting in the vertical direction. This allows us to write the *r* component of the force in a simplified form:

$$\begin{aligned} f_z &= -m_d\, g - q\phi'(z-h(r)) = 0\,, \\ f_r &= h'(r)\, q\phi'(z-h(r)) = -h'(r)\, m_d\, g\,, \\ f_r &\approx -2c\, r\, m_d g \equiv -k\, r \quad . \end{aligned} \tag{13}$$

The constant $k = 2m_d\, g\, c = m_d\, g / R_c$ is a harmonic restoring force constant for the lateral motion about the center of the potential well if it is parabolic. From detailed observations of the lateral motion of particles one can determine *k* and c.

The particles are found to be arranged in an hcp (hexagonal close packed) lattice for the most part. The crystal is not perfect however, as the compression forces the density to be larger at the center than at the perimeter of the disk. Thus there are several defects within the lattice. Knowing this, we can simplify the analysis of the balance between the repulsive pair interaction potential and the applied compressive force. The theory that we derive in this section is a continuum mechanics limit of the discrete particle layer. Let *s(r)* denote the nearest-neighbor (nn) spacing in the hcp lattice, where the radius is written to acknowledge that the average spacing will vary within the disk-like layer. It is easy to show that the areal number density is related to the hcp nn spacing by:

$$n = 2/\sqrt{3}\, s^2 = 1.1547/s^2 \tag{14}$$

on the average at any point within the crystal.

We will take the pair-wise interaction potential between the particles to be a spherically symmetric function of the separation, $V_{pair}(r)$. Because the particle layer lies within a plane, the interaction is really only being assumed to be azimuthally symmetric about the vertical axis. The potential energy per particle within an hcp lattice is $3V_{pair}(s)$ when nn interactions dominate. From this one can see that the potential energy density within the layer is given by:

$$e(r) = 3n(r)V_{pair}(s(r)) \tag{15}$$

which is in units of J/m^2 since we are in a 2D geometry.

From the steady-state Euler equation giving the momentum relation for a continuum fluid, or just from simple addition of forces, one can argue that the radial equation relating the pressure $p(r)$ and external force applied to the layer is just:

$$\begin{aligned} dp(r)/dr = F_r(r) &= n(r)\, f_r(r)\,, \\ &= -\,n(r) m_d\, g\, h'(r)\,, \\ &\approx -\,k\, r\, n(r)\,, \end{aligned} \tag{16}$$

where F_r is the force per area within the layer and f_r is the force on an individual particle as given in Eq.(13). The parabolic approximation enables several simple relations to be derived relating pressure to particle density variation, but that will not be pursued until later.

What is still needed is the relation of pressure to the individual pair-wise forces within the layer. This can be worked out by the following analysis. Consider a small areal element of the lattice at some radius. Let the area be A, with N particles within A. The number density is $n = N/A$. We know that pressure is defined by the change in energy with volume, or with area in this two-dimensional case. This relation is $dE = -pdA$, from which we can solve for p using Eq.(15) and the definitions of A and n. This gives:

$$\begin{aligned} p &= -\frac{dE}{dA} = -\frac{d(Ae(s))}{d(N/n(s))} = -\frac{d(3NV_{pair}(s))}{N\,d(\sqrt{3}s^2/2)} \\ &= -\sqrt{3}\,\frac{dV_{pair}(s)}{s\,ds} \end{aligned} \tag{17}$$

This relation applies at any radius r within the layer where the local pressure is $p(r)$ and the nn separation is $s(r)$. However it can only apply at the disk outer radius if the nn separation s is allowed to become infinite just beyond $r = r_M$, where r_M is the radius of the last ring of particles in the dust layer. This is consistent with zero density for $r > r_M$. As $r \to r_M$ from smaller values, both $s(r)$ and $n(r)$ approach non-zero values. The appropriate boundary condition for the *outer set of particles* at the perimeter of the dust layer can be found by balancing the inward force due to the external field with the vector sum of the pair-wise forces with the next inward group of particles. This leads to an approximate relation depending on the particle arrangement in the outer layer. The force balance relation is:

$$\sqrt{3}\,V'_{pair}(s_M) = f_r(r_M) \approx -k\,r_M \tag{18}$$

which is assuming an ideal crystal structure at the perimeter. In the limit of a minimum configuration of seven hcp particles, the $\sqrt{3}$ factor in this equation would become a factor of 2.

We can now combine Eqs.(16) and (17) to give a balance equation for the pressure within the layer:

$$\frac{dp(r)}{dr} = -\sqrt{3}\,\frac{d}{dr}\,\frac{dV_{pair}(s)}{s\,ds} = n(r)\,f_r(r) \quad , \tag{19}$$

in which *s* is implicitly a function of *r*. The first integral can be found, using the relation of n to s written in Eq.(14) and the expression for the radial component of the force given in Eq.(13):

$$\begin{aligned} \left[s\frac{dV_{pair}(s)}{ds} - 2V_{pair}(s) \right]_{s_o}^{s} &= -\frac{2}{3}\int_0^r dr'\, f_r(r') \\ &= \frac{2}{3} m_d\, g\,(h(r) - h(0)) \end{aligned} \quad , \tag{20}$$

where the superscript and subscript on the square brackets indicate that the expression contained within is to be evaluated as $\left[f(x) \right]_a^b = f(b) - f(a)$. Eq.(20) can be useful as it stands. Boundary conditions have been applied such that $r = 0$ corresponds to nn separation $s = s_o$ at the center of the layer. As $s \to s_M$, where s_M is the maximum pair-wise separation within the layer, *r* approaches the radius of the disk, r_M. This expression for r_M is a function of s_o, reflecting the fact that the compression of the layer at the center depends on the size and cumulative weight of the layer. This can only be determined by an integration of the differential relation connecting *r* and *s*.

The differential equation determining the variation of properties within the layer is found from Eq.(20) by reverting to the differential form for the Euler momentum equation. The equation is:

$$\frac{ds}{dr} = \frac{2}{3} m_d\, g\, \frac{h'(r)}{sV''_{pair}(s) - V'_{pair}(s)} \tag{21}$$

This is a highly non-linear ordinary differential equation with a moveable singularity for typical choices of the pair interaction. The boundary condition at zero radius will determine where the singularity occurs, which is somewhat beyond the location of the boundary of the particle layer, r_M. The necessity of doing a numerical solution for $s(r)$ is the price one pays for having an unspecified pair potential as well as a general form for the confining potential.

As an example of the usefulness of Eq.(21), we show the solution compared to experimental data in Fig.1. The dust layer was formed from 8.3 μm diameter melamime particles in an rf-driven Ar plasma. The electrode radius of curvature was 0.5m and this was verified to be the curvature of the dust layer itself. Eq.(21) was started with $s_o = 0.51\,mm$, and the Debye screening length and charge were fixed at 260 μm and -23500 *e*. The experimental data represents a collection of all nn separations within the dust layer, from the center of the nearly circular dust layer to the perimeter. The Debye parameters were determined from additional analysis of the experimental data in a plasma of the identical properties. The termination of the $s(r)$ curve was fixed by boundary conditions to be given later.

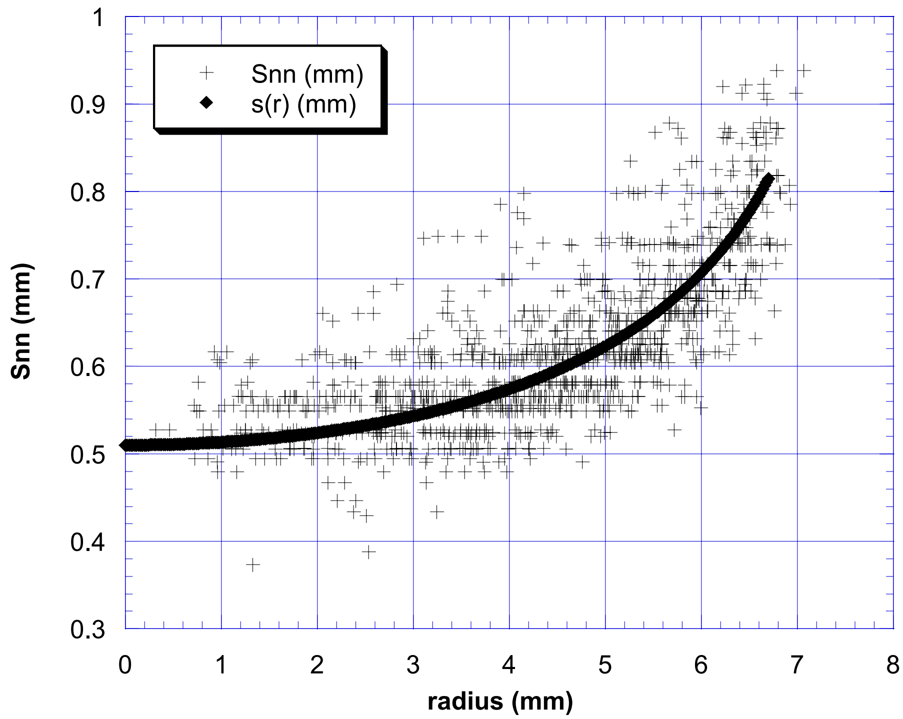

Figure 1. Comparison of theory (thick curve) with experimental data (+) taken from a dust layer in a spherical (parabolic) electrode of 0.5 m radius of curvature. The screened Coulomb Debye potential has a screening length of 260 μm and a charge of -23500 electron units. The only free parameter to enter the theoretical equation of state was the nn separation at the center, 0.51 mm, which can be determined from the experiment. The termination of the theoretical curve was determined by Eq.(18).

3.A Special forms of equation of state for a parabolic confining well

If the r-dependent shift of the plasma field is quadratic as indicated in the last equation of Eq.(5), we can write some especially simple formulae for the relation of the pair interaction to the total number of particles trapped in a monolayer disk. In Eq.(19) introduce $f_r = -kr$ on the right side and integrate from $r = 0$ to r. This gives:

$$p(r) - p(0) = -\frac{k}{2\pi} N_<(r) \tag{22}$$

where $N_<(r)$ is the number of particles within radius *r*. Allowing the radius to become larger than the radius of the disk reveals that:

$$p(0) = -\sqrt{3} \left. \frac{dV_{pair}(s)}{s\,ds} \right|_{s=s_o} = \frac{k}{2\pi} N_{total} \tag{23}$$

where we have used the result given in Eq.(17) and defined N_{total} as the total number of particles in the disk. Of course s_o is the nn spacing at the center of the disk.

3.B Special form of the pair interaction

As an example, we can choose the nn pair interaction to be a Debye-shielded inverse power potential:

$$V_{pair}^{(n)}(r) = \frac{A}{r^n} \exp(-r/\lambda) \quad . \tag{24}$$

Limiting forms of this potential include the Coulomb potential, the aligned dipole-dipole repulsion, and the unshielded potentials. Evaluation of Eq.(20) with a parabolic form for $h(r)$ gives:

$$r^2(s) = \frac{3}{k}\left[(n+2+\frac{s}{\lambda})\ V_{pair}^{(n)}(s) \right]_s^{s_o} \tag{25}$$

using the same notation for the brackets as in Eq.(20). If we label the point in radius where the nn separation becomes infinite as r_∞, we see that r_∞ is given by

$$r_\infty^2 = \frac{3}{k}(n+2+\frac{s_o}{\lambda})\ V_{pair}^{(n)}(s_o)\,. \tag{26}$$

The singular point r_∞ where $s \to \infty$ occurs at a point in radius greater than r_M. An approximate connection of r_∞ and r_M can be found to be:

$$r_\infty \approx r_M + s_M\sqrt{3}/2\,. \tag{27}$$

This would enable a least-squares' fit of the observed maximum radius as a function of s_o in terms of the parameters contained in the pair interaction potential.

We want to infer properties of V_{pair} from experimental observations of the variation of $s(r)$, or, at the minimum, from observations of $s_o = s(0)$ as it varies with r_M or the total number of particles in the layer N_{total}. The best we can do for this special form of the pair interaction is to write the equation resulting from Eq.(23):

$$\sqrt{3}\frac{1}{s_o}\left(\frac{n}{s_o}+\frac{1}{\lambda}\right)V_{pair}^{(n)}(s_o)=\frac{k}{2\pi}N_{total} \tag{28}$$

which enables a graphical analysis of available data for nn spacing at the center versus the total number of particles.

The utility of Eq.(28) in fitting experimental data is illustrated in Fig. 2. In this case we set $n=1$ to correspond to a Debye-screened Coulomb interaction and determined the best screening length and charge to enable Eq.(28) to fit the observed center spacing. The experimental data is taken from dust crystalline layers of various sizes in a confining electrode of $R_c = 0.5\,m$. The fitting analysis gave an effective dust charge of -23400 *e* and a screening length of 249 μm.

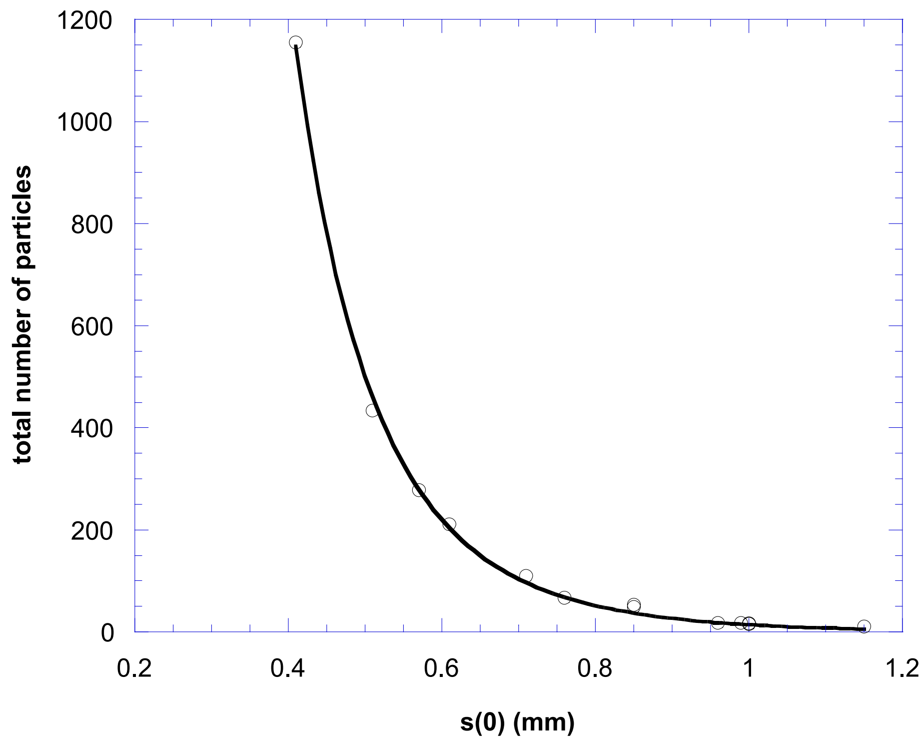

Figure 2. Least-squares fit of Eq.(28) to data taken with a spherical (parabolic) electrode of 0.5 m radius of curvature. The total number of dust particles is called N_{tot} and is the total particle count in the circular dust layer. *s(0)* is the nn separation of the particles at the center of the layer.

4. Single particle trajectory analysis to determine well curvature

In order to determine the curvature of the confining well produced by the shift in sheath height, $h(r) \approx cr^2$, we must observe the "slide" of a single particle as it falls into the center of the bottom electrode region. $h(r)$ or the constant c embed details of the multidimensional aspects of the plasma for a particular power, electrode geometry, plasma gas, dust particle size, electron temperature, and so on. All these properties must be maintained constant in order that $h(r)$ does not change in moving from the single particle analysis to the analysis of the multi-particle layer as given in the previous Section 3. The important point is that we *isolate the confining force* by observing a single particle trajectory and use this force to analyze the compression of the multi-particle layer of dust.

Particle trajectories that fall into the layer from above necessitate all the details of the dynamics presented in Section 2. However, once the particles have been trapped in the pre-sheath or sheath layer, their motion is confined to the nearly planar region of the disk that forms from many particles. In this two-dimensional region, a single particle sees only the weak, nearly horizontal, forces due to gravity and the viscous drag due to motion with respect to the background neutral gas. The ion wind force (slightly non-vertical) is perpendicular to the motion and does not accelerate the particle once trapped. The thermophoretic force $\vec{f}_{tp}$ is likewise assumed to be perpendicular to the electrode and the layer of trapped ions. It is to be noted that the analysis of the pair-wise interaction does not really depend upon these forces being exactly perpendicular to the horizontal motion in the disk layer. Whatever force is observed to cause the single particle motion into the confining well will also be operative in the many-particle layer. The only assumption is that the plasma does not change character with the addition of many particles. We have found experimentally that we can use a curved electrode such that the plasma sheath adjusts conformally to the surface. In this case, we have an experimental check on the value of R_c for the layer.

In this two-dimensional sheet we can approximate the Newtonian equation of motion as:

$$\begin{aligned} m_d \ddot{\vec{r}} &= -m_d \gamma_{gas} \dot{\vec{r}} + \hat{e}_r f_r \\ &= -m_d \gamma_{gas} \dot{\vec{r}} - \hat{e}_r m_d g h'(r) \\ &\approx -m_d \gamma_{gas} \dot{\vec{r}} - \hat{e}_r k r \end{aligned} \tag{29}$$

where f_r has been given in Eq.(13). If the angular momentum of the particle has damped sufficiently we may replace this 2D equation with the one-dimensional equation in Cartesian coordinate x. This becomes a simple damped oscillator equation, which is harmonic if $h(r)$ is parabolic:

$$\begin{aligned} \ddot{x} &= -\gamma_{gas} \dot{x} - g h'(x) \quad , \\ \ddot{x} &\approx -\gamma_{gas} \dot{x} - \omega^2 x \quad , \\ \omega^2 &= k / m_d \quad . \end{aligned} \tag{30}$$

The harmonic case can be analyzed by substitution of an exponential, $x = \exp(\alpha t)$, showing the usual oscillatory, damped, and intermediate behavior. The simple interesting result is for damped motion in which a plot of the ratio of velocity to position should give the desired constants:

$$\begin{aligned} -\dot{x} / x &= \omega^2 / \gamma_{gas} = (k / m_d) / \gamma_{gas} \\ &= 2 c g / \gamma_{gas} = g / R_c \gamma_{gas} \end{aligned} \quad . \tag{31}$$

Whether this limit alone is adequate, or one needs to do a comparison to the full damped oscillator solution, must be evaluated for a particular pressure and curvature.

5. Computer Simulation of Brownian Motion

The small dust particles being treated in this study are more massive than individual atoms and ions by more than twelve orders of magnitude. They are visible to the unaided eye with the proper illumination and are candidates for a Brownian motion analysis. The frequency of individual atomic collisions with the particles is much too high to include within a "molecular dynamics" treatment of the particles. Nevertheless one can simulate the stochastic nature of the collisions and produce the same effect. We use the "partial velocity reset" method[6] to do this simulation in the context of a numerical solution of the Newtonian equations of motion (NEOM) for the particles.

As the stochastic gas collisions are to be included by this algorithm, we integrate the NEOM for a particle, or for many, as written in Eq.(1), but *without* the gas-damping coefficient γ_{gas}. At small appropriate intervals, the numerical integration of the NEOM is stopped and all particle Cartesian velocity components v_i are reset discontinuously to new values:

$$v_i^{new} = (1-\theta)^{1/2}\, v_i^{old} + \theta^{1/2}\, v^T(\xi)\,, \tag{32}$$

where $v^T(\xi)$ denotes a random velocity selected from a Maxwellian distribution at temperature T. ξ labels the random sequence of numbers defining the velocity components at this reset time. The parameter θ in Eq.(32) can be related[6] to the interval Δt between application of the reset and the damping coefficient γ_{gas}:

$$\theta = 2\,\Delta t\,\gamma_{gas}\,. \tag{33}$$

The physically correct value of γ_{gas} is known from other analysis as discussed in Section 2.A. Obviously we must reset the velocities frequently enough to have $\theta < 1$. We note that the partial velocity reset procedure consistently describes the balance between viscous damping of the motion as well as the Brownian thermal agitation.

It is possible that experimental observations of the Brownian motion can be matched to the simulations in order to check the consistency of dust size, gas density, gas temperature, and kinetic dust temperature. For example, if a dust particle is at equilibrium with a Boltzmann distribution at a translational temperature T_d in a parabolic well characterized by a radius of curvature R_c, the probability distribution with radius is:

$$
\begin{aligned}
P(r) &\propto \exp(-(r/w)^2)\,, \\
w^2 &= 2R_c\, kT_d / m_d\, g\,.
\end{aligned}
\tag{34}
$$

The HWHM (half width at half maximum) of the spatial distribution is related to *w* by $w_{HWHM} = w\sqrt{\ln 2}$. This should be a good confirmation of the dust *and* gas temperature and well curvature that is *independent* of the details of the scattering from the surface of the particle, which affects γ_{gas}. A material temperature of the dust particle that is very different from the kinetic temperature will cause non-equilibrium and invalidate the assumptions in the probability distribution. It is also true that the ion collision rate with the particles will affect their translational temperature, but as long as the plasma density is typically low compared to the neutral density, this effect is small.

In Fig. 3 we illustrate the motion of a typical dust particle over a period of 30 s in Ar gas at 300 K. The trajectory has not had sufficient time to fill out the spatial profile in the confining parabolic potential which has $R_c = 0.5\,m$. The motion in the vertical direction is likewise Brownian-like, with a distinct random walk. A much longer solution of the NEOM of the particle shows that the spatial distribution develops the gaussian profile in space as given by Eq.(34).

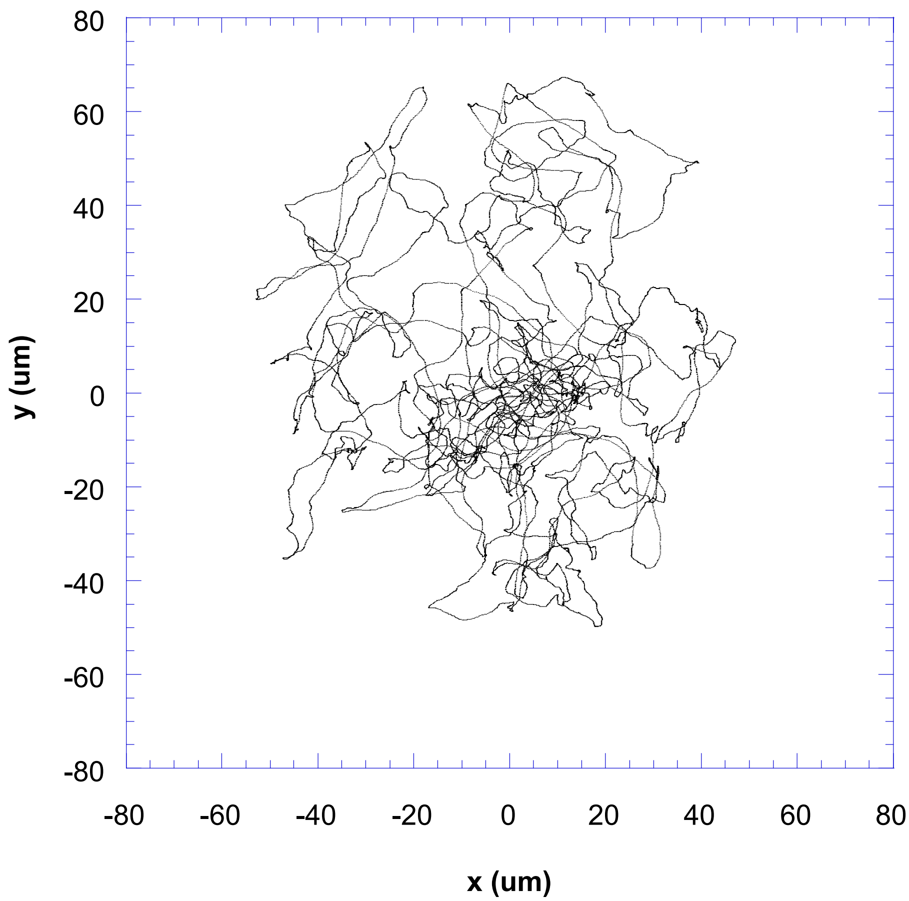

Figure 3. Random walk of a dust particle in the x-y plane of a confining well calculated by the partial velocity reset method of Riley, Coltrin, and Diestler.[6] The gas temperature is 300 K and the period of integration is 30 s.

Within certain limits, the particle velocity distribution should be Maxwellian in any shape of confining field, and this can be used to infer the particle temperature. The spatial distribution, if measured directly, can be used to infer the shape of the confining field if the temperature is known. It is the hope here that Brownian motion will give some handle on the issues of neutral gas temperature, particle translational temperature, and possibly ion-excited temperature of the particle and spatial variations in the confining fields.

It is seen from the calculations that the particle establishes a thermal velocity distribution quickly, but that the spatial distributions take much longer to develop due to the slow diffusion in real space.

7. Conclusions

Hopefully the equation-of-state model and the theoretical analysis contained within will be of general help in the determination of the pair interaction potential for plasma dust particles. The example cases presented herein are being prepared for publication elsewhere. It is hoped that the Brownian motion analysis will be useful in characterizing the local environment of the particles.

Acknowledgment

We acknowledge discussions with Rick Buss and Pauline Ho, who first noticed the compressibility of plasma dust layers. We also thank John Torczynski and Dan Rader for help with the characterization of thermophoretic forces on dust particles.

This work was supported by the U. S. Department of Energy under Contract DE-AC04-94AL85000 at Sandia National Labs. Sandia is a multiprogram laboratory operated by Sandia Corporation, a Lockheed Martin Company, for the United States Department of Energy.

References

[1] M. E. Riley, "Dust in the Ion Wind: A Model for Plasma Dust Particle Dynamics," Sandia National Labs Tech. Report SAND2001-0406, Feb. 2000.

[2] P. S. Epstein, Phys. Rev. (Series 2), **23** 710 (1924).

[3] M. A. Gallis, J. Torczynski, and D. J. Rader, Phys. Fluids, in prep. 2001.

[4] M. A. Gallis, D. J. Rader, and J. Torczynski, Aeroso Sci. and Tech., in prep., 2001.

[5] J. E. Allen, Phys. Scr. **45** 497 (1992), with first usage in H. M. Mott-Smith and I. Langmuir, Phys. Rev. **28** 727 (1926).

[6] M. E. Riley, M. E. Coltrin, and D. J. Diestler, J. Chem. Phys., **88** 5934 (1988).

DISTRIBUTION:

2	Professor J. Goree Department of Physics and Astronomy University of Iowa Iowa City, Iowa 52242	
2	Professor G. E. Morfill Max-Planck-Institut fur Extraterrestrische Physik 85740 Garching Germany	
2	Professor Mark Kushner Electrical and Computer Engineering University of Illinois Urbana, IL 61801	
1	MS 0836	Richard J. Buss, 09117
1	MS 0827	Robert B. Campbell, 09117
10	MS 1423	Greg A. Hebner, 01118
1	MS 0601	Pauline Ho, 01126
1	MS 1186	Barry M. Marder, 01674
1	MS 1423	Paul A. Miller, 01118
10	MS 1423	Merle Riley, 01118
1	MS 9018	Central Technical Files, 8945-1
2	MS 0899	Technical Library, 9616
1	MS 0612	Review & Approval Desk, 9612 [For DOE/OSTI]